applied sciences

MDPI

Article

Surface Discharge Mechanism on Epoxy Resin in Electronegative Gases and Its Application

Herie Park [1], Dong-Young Lim [2] and Sungwoo Bae [3,*]

1. Division of Electrical and Biomedical Engineering, Hanyang University, 222 Wangsimni-ro, Seongdong-gu, Seoul 04763, Korea; bakery@hanyang.ac.kr
2. Hyundai Technical High School, 122 Mipo-ro, Dong-gu, Ulsan 44032, Korea; dylim@hcu.hs.kr
3. Department of Electrical Engineering, Hanyang University, 222 Wangsimni-ro, Seongdong-gu, Seoul 04763, Korea

* Correspondence: swbae@hanyang.ac.kr; Tel.: +82-2-2220-2309

Received: 26 August 2020; Accepted: 23 September 2020; Published: 24 September 2020

check for updates

Abstract: This study presents the surface discharge characteristics of insulating gases, including sulfur hexafluoride (SF_6), dry air, and N_2, under a non-uniform field. Surface discharge experiments were conducted, with the gas pressure ranging from 0.1 to 0.6 MPa, on samples of epoxy dielectrics under an AC voltage. The experimental results showed that the surface insulation performance significantly improved in insulating gases possessing electronegative gases, such as SF_6 and dry air. Surface flashover voltages of SF_6 were saturated with an increasing pressure, compared to dry air and N_2. The surface discharge mechanism is proposed to explain the improvement and saturation of dielectric characteristics of the electronegative gas in complex dielectric insulations, as well as its influence on the surface flashover voltage. As an application, an insulation design method is discussed with regards to replacing SF_6 gas in high-voltage power equipment based on the knowledge of the physics behind gas discharge.

Keywords: surface discharge; epoxy resin; electronegative gas; high-voltage power equipment

1. Introduction

Sulfur hexafluoride (SF_6) plays an important role as an insulating gas in high-voltage power equipment. More than 80% of SF_6 produced worldwide is supplied for use in high-voltage gas circuit breakers, gas-insulated switchgears, and gas-insulated lines, due to its exceptional physical and chemical properties, including its high dielectric strength, current interruption performance, thermal conductivity, thermal stability, nonflammability, nontoxicity, and non-explosive characteristics [1–4].

Despite the outperformance of SF_6, its use in power equipment is becoming increasingly dangerous owing to its high global warming effect, its long atmospheric lifetime, and the high toxicity of decomposed byproducts that result in many environmental problems. The global warming potential (GWP) of SF_6, relative to CO_2, over a 100-year time horizon is 23,500. This means that the global warming effect of 1 kg of SF_6 gas is equivalent to that of 23.5 tons of CO_2 in the atmosphere. Considering that the global annual emission of SF_6 was 8100 tons in 2012, which is equivalent to annual greenhouse gas emissions of approximately 185 million tons of CO_2, its overall GWP impact is not marginal compared to that of CO_2 [5]. Owing to its high greenhouse effect, the European Union intends to reduce the SF_6 sales of 2014 to one-fifth by 2030 [6]. The California Air Resources Board (CARB) has proposed stricter requirements governing the use of SF_6, including phasing out its usage in gas-insulated equipment and further reducing allowable greenhouse gas (GHG) emissions from such equipment from 2020 onwards [7]. Moreover, the decomposition products are produced by the electrical and thermal decomposition of SF_6 in the presence of other molecules, such as H_2O, SiO_2, N_2, O_2, H_2, and Ar.

It should be noted that the products containing fluorine and/or sulfur in SF_6 decomposition, including as S_2F_{10}, SF_4, and hydrofluoric acid (HF), are highly reactive, corrosive, and toxic. These are also potent GHGs [8].

Therefore, to reduce its use, many replacements for SF_6 have been investigated for application in high-voltage power equipment. These investigations have focused on using common gases (CO_2, N_2, and dry air), halogenated gases (CF_3I, hydrofluoroolefins (HFOs), and perfluorinated compounds (PFCs)), and mixture gases as substitutes for SF_6. Their dielectric strength and characteristics have been compared with those of SF_6 [9]. In addition to gas insulation, composite insulation has been applied to SF_6-free gas-insulated switchgear (GIS), instead of simple dielectric insulations by vacuum, gases, or solid dielectrics [10,11]. Composite insulation is a method of using a solid dielectric and an insulating gas together. However, composite insulation comes with problems of deterioration in the insulation performance of the equipment, due to the use of a solid dielectric. The insulation performance deteriorates owing to the formation of a triple junction or a surface discharge. The triple junction induces a high electric field in the region where an electrode is in contact with both the insulating gas and the solid dielectric. Surface discharge is undesired gas breakdown that occurs on a surface at a high voltage, lower than the breakdown voltage of the insulating gas. This breakdown is attributed to the weak point of the dielectrics used and their interactions within the power equipment [10,12,13].

To design a composite insulation for SF_6-free power equipment, it is necessary to investigate the fundamental surface discharge characteristics of the composite insulation and identify its weaknesses. Extensive research has been conducted on the surface discharge mechanism in different materials under different electric fields formed by AC, DC, and impulse voltage [10,14–16]. Béroual et al. [10,14,15] presented the experimental characterization of discharge propagation over insulators such as Bakelite, epoxy, and glass immersed in a single gas or mixture gas, under lightning impulse, DC, and AC voltages. The shape and length of creeping discharge patterns were investigated to understand the capacitive charge effect and electric field influence. Kato et al. [16] conducted experiments under a negative impulse voltage to clarify the surface flashover characteristics based on the existence of surface charges on an alumina insulator in a vacuum. The influence of surface charges on the electric field and the secondary electron emission avalanche were explained. These investigations have succeeded in revealing that the surface charges of insulators influence the surface flashover characteristic.

In order to investigate the occurrence of surface flashover, the effects of the gas medium and its pressure, thickness and dielectric constant of a solid insulator, roughness and shape of the electrode, and applied voltage on gas breakdown have been further explored [3,17–21]. These investigations have reported that surface flashover occurs at the triple junction and in its vicinities in several common and specified factors influencing the surface discharge [19]. Park et al. [3] compared the surface discharge characteristics of different gas media, such as SF_6, N_2/O_2 mixture gases, and imitation air, and explained the important role of the O_2 concentration in the N_2/O_2 mixed gas. Lim et al. [19] conducted a comparative study on SF_6 alternative candidate gases for investigating the surface insulation performance of eco-friendly gas, including N_2/O_2 mixture gas, dry air, and compressed air under AC voltage. Based on the experimental results and the comparative study, the effect of moisture contained in the candidate gases and the correlation among the electric filed intensity, collision-ionization coefficient, electron attachment coefficient, and gap length were discussed. Douar et al. [20] presented the ignition of surface discharges and their propagation governed by repulsion due to electrostatic force and attraction caused by nonlocal photo-ionization.

Before the occurrence of surface flashover, the solid dielectric causes the occurrence of physical phenomena, such as electron emission at a triple junction, surface charge accumulation, photoemission, and a secondary electron emission avalanche (SEEA). These phenomena contribute to electron avalanches and the formation of a conductive channel on the dielectric surface. There are several surface discharge mechanisms, based on electron generation and the high electric field as a physical phenomenon in a vacuum [16,18,22]. However, this physical phenomenon and the detailed progression of surface discharge have not yet been fully understood in compressed gases with various electronegative gases. This means that prior research dealing with the progression and suppression of surface discharge is rather limited, in terms of the detailed physical processes of electron generation and disappearance in compressed gas. Although the authors have studied the effect of the concentration of O_2 on surface discharge characteristics in compressed gas in previous works [3,19], many studies on surface discharge seem to be carried out under vacuum or gases with a pressure of 0.3 MPa or less. This research trend has led to a gap in knowledge about the detailed mechanism by which an electronegative gas among high-pressure gases generates electrons during the surface discharge process. This knowledge gap means that the surface insulation design of SF_6-free high-voltage equipment with high-pressure compressed gas is still a challenging problem. In this paper, we analyze the effect of SF_6 and O_2 in compressed gas on electron generation during the surface discharge progress, and provide useful physical information for the surface insulation design of high-pressure SF_6-free high-voltage equipment.

This study describes the surface discharge characteristics of epoxy resin in compressed gases (i.e., SF_6, dry air, and N_2) under a non-uniform electric field. It aims to understand the solid-gas composite insulation characteristics and analyze the effect of secondary electron attachment emitted from the dielectric surface on the surface insulation performance. The reason for the excellent surface insulation performance of electronegative gases (SF_6 and dry air) is explained in detail in this paper, based on the physics governing the gas discharge and the surface discharge mechanisms.

The remainder of this paper is organized as follows. The experimental setup and experimental procedure are introduced in Section 2. The experimental results of the surface discharge characteristics in compressed gas dielectrics are presented in Section 3. The surface discharge mechanism and the insulation design method of an SF_6-alternative insulating gas, based on the effect of the electronegative gases and electron swarm parameters, are discussed in Section 4. Finally, conclusions are presented in Section 5.

2. Experimental Setup and Method

A parallel needle-plane electrode system enclosed in an experimental gas-insulated switchgear (GIS) filled with different gases was used in this study. The specifications of the electrodes used in this experiment are as follows: The needle electrode (*N*) had a diameter of 5 mm and 20° angle of a point (θ). The diameter of the plane electrode (*P*) was 59 mm. Both electrodes were made of stainless steel and were arranged vertical to each other. The solid dielectric used was made of epoxy resin and was in the form of a disc with a diameter (d) of 100 mm and a thickness (t) of 2 mm. The sample of epoxy resin was inserted between the electrodes. The distance between the epoxy dielectric and the needle electrode was zero, and the needle electrode was carefully contacted, without damaging the epoxy surface, since damage to the epoxy surface affects the surface flashover voltage. Figure 1a illustrates a schematic diagram of the experimental electrodes and a solid dielectric arrangement.

The experimental gas-insulated switchgear (GIS) chamber is shown in Figure 1b. This chamber is made of stainless steel of a 20 mm thickness and consists of two layers: An interior part with a diameter of 260 mm, height of 460 mm, and volume of 25 L, and an exterior part with a diameter of 460 mm, height of 500 mm, and volume of 83 L. Two windows were used to observe the inside of the experimental chamber. These windows were made of acryl with a diameter of 110 mm and thickness of 20 mm. The chamber was designed and manufactured to endure a fixed temperature range (−90–100 °C) and pressure up to 1.0 MPa. It was also capable of withstanding an AC voltage of 300 kV. A pressure gauge was installed to measure the pressure inside the chamber. The chamber could be preserved at a pressure of 6.67×10^{-2} Pa by using a vacuum pump (SINKU KIKO Co., Ltd. Miyazaki, Japan, GUD-050A).

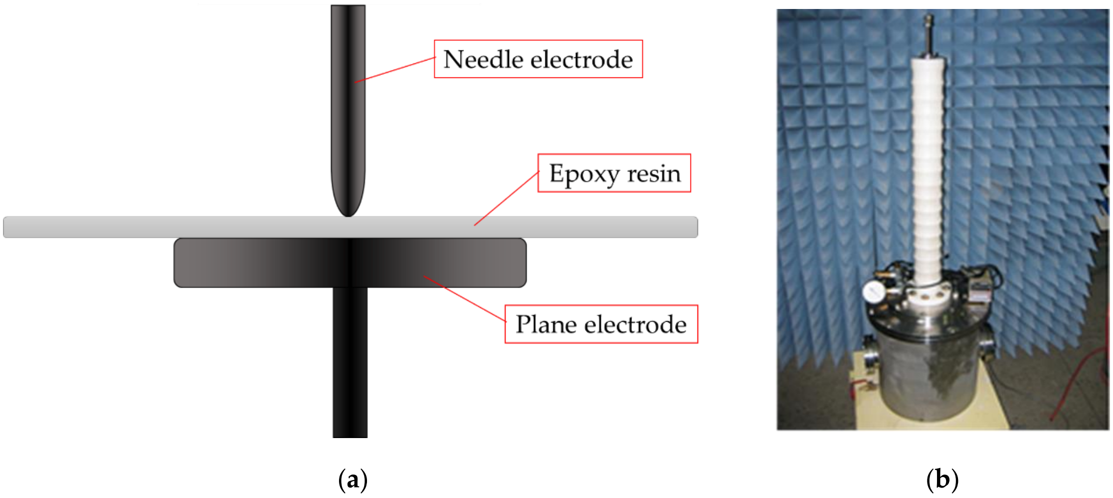

Figure 1. Experimental setup: (**a**) Scheme of the electrode arrangement and (**b**) the experimental GIS chamber.

The insulation gases used were SF_6, dry air, and N_2. Dry air was produced by a dry air production device. The device had three types of filters that could reduce impurities and lower the dew point of dry air. The final dew point of dry air produced using this device was less than −60 °C. These gases were pressurized from 0.1 to 0.6 MPa, inside the chamber of the device.

The experiments were performed under AC voltage supplied by a high-voltage generator (DY-106-Korea, AC 300 kV/120 mA) with a voltage rising speed of 3.15 kV/s. As an AC power source is actually used as the operating power of GIS, gas-insulated transmission lines (GIL), and gas circuit breaker (GCB), it is very important to analyze the surface discharge characteristics and mechanisms for the device and equipment working under AC power. After ventilation of the chamber to 6.67×10^{-2} Pa, each type of gas was inserted and pressurized from 0.1 to 0.6 MPa, inside the chamber. AC voltage was applied to the electrodes at each pressure level that the gases were subject to. Then, the surface flashover voltages were sequentially measured five times. The average value of this measurement is referred to as the mean surface flashover voltage (V_B) in this study. The surface flashover voltages were measured using a high-voltage probe.

3. Experimental Results

Figure 2 illustrates the surface flashover voltages of SF_6, dry air, and N_2, each at a gas pressure ranging from 0.1 to 0.6 MPa. From this, the effect of pressure on the surface flashover voltages and the breakdown voltages can be analyzed. These voltages increase monotonically with an increasing pressure of SF_6, dry air, and N_2. This monotonous rise is attributed to a shorter mean free path with an increasing gas pressure. The short mean free path limits the acceleration of electrons and reduces the number of electrons with high kinetic energy between the electrodes. The limitation and reduction suppress collision ionization and the SEEA, and such suppression results in an increase in the breakdown voltage and surface flashover voltage. An interesting observation in Figure 2 is the surface discharge characteristic of SF_6. The insulation characteristics of electronegative gases such as SF_6, under a non-uniform electric field, are a clear *N*-shaped breakdown voltage. This *N*-shape rises after the breakdown voltage decreases with an increase in pressure [23,24]. The *N*-characteristic has also been observed in N_2/SF_6 mixed gas containing 0.1% SF_6 [24]. However, the *N* characteristics were not revealed in this study. The corona stabilization effect due to positive space charges leads to *N*-shaped properties. It is presumed that the unobserved *N*-characteristic in this study is due to the weak corona stabilization effect, because of the different experimental conditions employed by other researchers [23,24]. The most evident difference between the references [23,24] and our experiment is the presence of a solid dielectric. The existence of the solid dielectric may strongly influence the distribution of positive ions between electrodes. The mechanism of surface discharge in our electrode system with a solid dielectric would be different from the mechanism of breakdown in an electrode system without any dielectric. The dominant mechanism of surface discharge is the SEEA from the solid dielectric, while that of breakdown manifests as additional avalanches due to positive space charges.

The solid dielectric placed between electrodes plays an important role as an electron source that emits electrons through electron collision and photon irradiation on the surface of the dielectric. Therefore, the dielectric leads the electron generation mechanism, including SEEA and photoemission, while developing surface discharge over the solid dielectric. In contrast, this electron generation mechanism does not occur in the breakdown mechanism under the electrode system without any solid dielectric between electrodes.

Figure 2 shows that the surface flashover voltage measured with a solid dielectric is higher than the breakdown voltage of the electrode system without any solid dielectric. In general, as the solid dielectric forms a triple junction point with a high electric field and electron sources, it is known that the surface flashover voltage is lower than the breakdown voltage. However, our experimental results showed the opposite. This is because the diameter of the solid dielectric is considerably larger than that of the plane electrode in our electrode system.

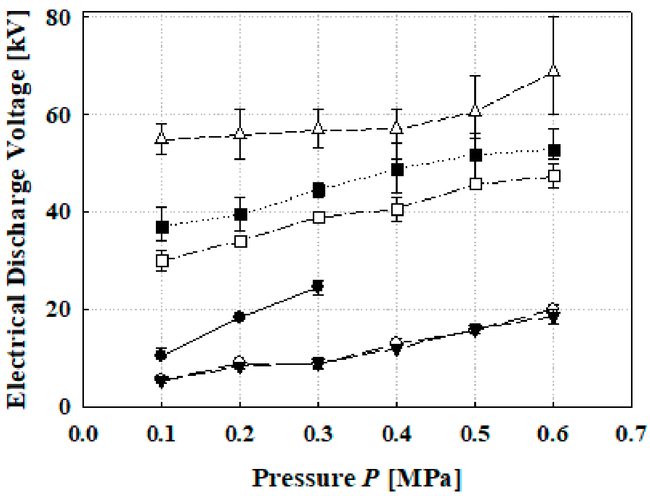

Figure 2. Surface flashover voltage (Δ, SF_6; ■, dry air; and □, N_2) and breakdown voltage (•, SF_6; ○, dry air; and ▼, N_2).

The surface insulation performance and the rate of increase in surface flashover voltages with an increasing pressure are noticeably different for electronegative gases (i.e., SF_6 and dry air) and the non-electronegative gas (i.e., N_2). The surface insulation performance of SF_6 and dry air was better than that of N_2 in the gas pressure range of this experiment. SF_6, being an electronegative gas, demonstrated a higher surface insulation performance than that of dry air. The excellent surface insulation performance of electronegative gases (SF_6 and dry air) is due to the electron attachment mechanism. Although both SF_6 and dry air are electronegative gases, the difference in the surface insulation performance between these gases was possibly due to the electron attachment cross section, which represents the electron attachment capability of gases. Saturation of the surface flashover voltages with an increasing pressure was observed in SF_6—evidently more than in dry air and N_2—within a gas pressure range of 0.1 to 0.4 MPa.

The rate of increase of the surface flashover voltage with an increasing pressure is shown in Figure 3. The insulating gas containing N_2 was insensitive to saturation in the pressure range. This saturation is presumed to be due to the electron detachment of negative ions in the electronegative gases (i.e., SF_6 and O_2) during surface discharge development. As N_2 cannot attach electrons, negative ions are not formed in N_2. This means that no electron detachment mechanism occurs in N_2. A detailed interpretation of the surface insulation performance and surface flashover voltage saturation will be explained in Section 4 based on surface discharge mechanisms.

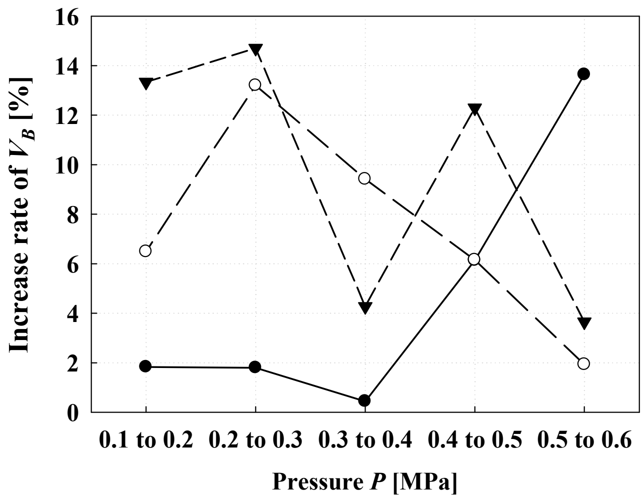

Figure 3. Rate of increase in the surface flashover voltages (•, SF_6; ○, dry air; and ▼, N_2).

4. Discussion

4.1. Surface Discharge Mechanism

This section describes the surface discharge mechanism in detail, explaining the experimental results presented in Section 3. The main outcomes were an improved surface insulation performance of insulating gases containing electronegative species and noticeable saturation of the surface insulation performance of SF_6 with an increasing pressure. These two results seem to be inherently related to the mechanisms of electron attachment and electron detachment, respectively, during the progression of surface discharge. The electron attachment is a mechanism by which SF_6 and O_2 trap electrons moving to the positive electrode to form negative ions between two electrodes. This reduces the number of electrons that cause collision ionization and the SEEA on the dielectric surface, thereby resulting in a higher surface insulation performance from the inclusion of an electronegative gas. However, the negative ions generated by electron attachment emit electrons from collisions among electrons, positive ions, and negative ions. As this electron detachment adds electrons between the electrodes, it may limit the rise of the surface flashover voltage.

Surface discharge is developed by an initial electron, the SEEA, a surface streamer, and conductive channel formation. The formation of an initial electron depends on the polarity of the applied voltage. When the applied voltage is positive, the initial electron is generated by the electron detachment of a negative ion around the needle electrode or electron emission from the epoxy surface. Examples of electron detachment from $SF_6{}^-$ ions can be presented as follows under an appropriate condition for each case [25]:

Collisional detachment: $SF_6^- + SF_6 \rightarrow SF_6 + SF_6 + e,$

Photodetachment: $SF_6^- + h\upsilon \rightarrow SF_6 + e,$

Thermally-induced detachment: $SF_6^- + heat \rightarrow SF_6 + e.$

When the applied voltage is negative, an initial electron is generated by field emission from the cathode at the triple junction, where the electrode, solid dielectric, and insulating gas make contact. This electron collides with the epoxy surface. Then, the generated initial electron contributes to the emission of secondary electrons from the surface. The secondary electrons again lead to an SEEA at the epoxy surface and collision ionization in the gas. During the process of collision ionization, photons emitted from the excited molecules are irradiated to both the epoxy surface and other molecules.

This irradiation results in photoemission and photoionization and can supply additional electrons in the discharge space between the electrodes. The electrons generated by field emission, the SEEA, ionization collision, photoemission, and photoionization can attach themselves to an electronegative gas.

During the development of surface discharge, negative ions can form from the electron attachment process. However, these ions can also disappear due to the electron detachment mechanism during the same surface discharge development. As the surface discharge develops with an increase in the applied voltage, the SEEA and photoemission can become more prominent. Owing to the active SEEA and photoemission processes, a surface streamer develops along the epoxy surface. The head of the streamer advances based on what the electron source is (photoionization/photoemission), and the surface streamer intersects between the electrodes. When a conductive channel is formed between the electrodes due to the surface streamer and the presence of many electrons, surface flashover finally occurs.

The most evident difference between an electronegative gas and a non-electronegative gas is the occurrence of electron attachment or detachment during the process of surface discharge development. The authors believe that these processes are the key determining factors that explain the experimental results. Electron attachment is the only process that removes electrons in the discharge space between electrodes in the surface discharge mechanism. The removal of electrons suppresses the formation of the streamer and conductive channels. This suppression is the reason behind the high surface insulation performance of an electronegative gas. Therefore, the surface insulation performance of the insulating gas containing electronegative gases SF_6 and O_2 is superior to that of N_2.

Although SF_6 and dry air are both electronegative gases, the disparity in the surface insulation performance between these gases can be explained by the difference in the electron attachment cross section, which determines the characteristics of the gases. Since the surface discharge grows on the surface of the epoxy dielectric, the capturing of electrons emitted from the surface appears to contribute to a significant improvement in the surface insulation performance. Electrons are generated from the epoxy surface during surface discharge by the SEEA and photoemission processes. The energy range of the electrons emitted from the surface by these processes was assumed to be 3.0–4.5 eV [16,26]. Figure 4 shows the electron attachment cross sections of SF_6 and O_2 in the electron energy range. Evidently, the cross section of SF_6 is considerably larger than that of O_2. From this figure, it can be assumed that the ability of secondary electrons, emitted from the epoxy surface, to attach themselves is significantly better in SF_6 than in O_2.

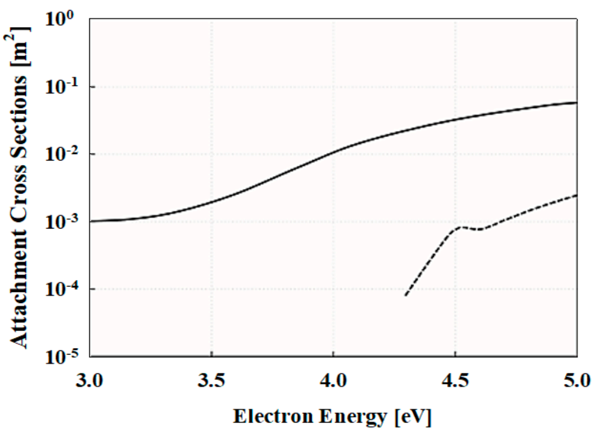

Figure 4. Attachment cross sections of gases (—, SF_6 and ---, O_2).

The progress of the streamer and the formation of a conductive channel on the epoxy surface can be suppressed by the capture (attachment) of the secondary electrons due to the large electron attachment cross sections. This could be the reason why SF_6, which has an excellent electron attachment ability in the electron energy range of 3.0–4.5 eV, exhibits a superior surface insulation performance compared to dry air [27].

In addition, the noticeable saturation of surface flashover voltages with an increasing pressure, in the pressure range of 0.1 to 0.4 MPa in SF_6, may be related to electron detachment. During surface discharge development, negative ions collide with electrons, positive ions, and other negative ions in the medium. Electrons attached to electronegative gas are then separated and detached from the negative ions by these collisions. The separated electrons are imbibed into the SEEA or collision ionization, helping the formation of a conductive path along the epoxy surface between the electrodes. In other words, a large number of negative ions can improve the surface insulation performance, and at the same time, can function as electron sources [28]. The electron detachment of negative ions mainly occurs from collisions with ions rather than high electric fields [29]. Since the mean free path becomes shorter as the pressure increases, it can be assumed that the collision of positive and negative ions also occurs more frequently with an increasing pressure. Frequent collisions activate electron detachment, causing a noticeable saturation of the surface insulation performance with an increasing pressure. The rise of the surface flashover voltage of SF_6 at 0.6 MPa may be related to a high-pressure surface discharge mechanism, such as leader discharge.

4.2. Insulation Design Method of an Insulating Gas Alternative to SF_6 Based on Electron Swarm Parameters

An insulation design method that can ensure a good insulation performance in high-voltage power apparatus such as GIS can be proposed from our experimental results, derived from Figure 2. The surface insulation performance can be enhanced by the inclusion of electronegative gases and an increase in the gas pressure. Therefore, these factors must be considered during insulation design. However, very rarely is apparatus designed with a gas pressure exceeding 1.0 MPa [23]; therefore, it is desirable to incorporate the addition of electronegative gases into the insulation design method.

An insulation design using a mixture of electronegative gases should be carried out upon analyzing the electron swarm parameters of the gases. These parameters are the electron attachment cross section and electron scattering cross section. The electron attachment cross section represents the ability of an electronegative gas to capture electrons. This ability depends on the energy of the electrons. There are certain energy ranges in which electronegative gases can effectively and easily capture electrons. In the discharge space, electrons accelerated by the applied electric field are distributed with various values of kinetic energy. The improvement in the insulation performance of the gas is attributed to the easy and effective capture of these electrons. Therefore, there is a need for a method of selecting an electronegative gas with a large electron attachment cross section spanning a wide range of electron energies. The lower the kinetic energy of the electrons, the easier the electron attachment is; thus, for insulation design, it is preferable to select an electronegative gas possessing a wide electron attachment cross section in a low electron energy range.

Meanwhile, the electron scattering cross section represents the ability to reduce the kinetic energy of electrons, which are accelerated by the applied electric field. This reduction of kinetic energy effectively activates the electron attachment of electronegative gases. Therefore, electron scattering results in high-energy electrons with the sufficient ionization capacity becoming inactive, consequently resulting in effective electron attachment.

Since the electron attachment process is more important than the ionization process in the prevention of a breakdown, only the addition of an electronegative gas is usually conducted in the insulation design method. However, for producing a higher insulation performance, the electron swarm parameters cannot be overlooked. Based on these two parameters (the electron attachment cross section and electron scattering cross section), the mixture gas that is more suitable for insulation design should include a gas with electron attachment abilities and the ability to suppress the electron behavior. It is preferable to include a mixture of two or more auxiliary gases with different electron attachment cross section peaks, depending on the electron energy, because one electronegative gas cannot capture all electrons in a considerably wide electron energy region. Meanwhile, the mixing of gases with an electron scattering capability that reduces the electron energy in the electron energy region corresponding to the peak of the electron attachment cross section should be recommended.

Based on these electron swarm parameters, the experimental results reported that the 2.5% positive lightning impulse breakdown voltage of SF_6/air and SF_6/CO_2 in 0.05 to 0.45 MPa under a non-uniform electric field with a gap of 10 mm is higher than that of pure SF_6 [30]. Kojima et al. [31] studied the insulation properties of a mixed gas containing two or more electronegative gases based on the electron attachment cross section, depending on the electron energy.

In addition to selecting the insulating gas, engineering techniques can be applied to an insulation design method, and these techniques should be integrated into high-voltage apparatus with a selection method of insulating gas that considers the electron swarm parameters. The engineering techniques are improvements in electrodes and solid dielectrics, details of which can be found in references [11,32–36]. The theoretical principles governing the engineering techniques are the suppression of electron generation and relaxation of the concentrated electric field. Since suppression and relaxation are the direct factors influencing gas breakdown, a good insulation performance can also be ensured with these engineering techniques. Therefore, when insulation gas selection and engineering insulation techniques are simultaneously applied to high-voltage apparatus, the surface insulation performance of the apparatus can be improved, owing to a synergistic effect that imbibes physical and engineering elements.

Therefore, the selection of insulating gas based on the physics of gas discharge (i.e., electron swarm parameters) is more important than engineering insulating design techniques. This is because engineering insulation design techniques are based on physical knowledge (i.e., physical mechanisms and physical analysis), while the insulation performance of the high-voltage apparatus is significantly dependent on the insulating gas. To date, single or mixed insulating gases that can completely replace SF_6 in terms of insulation, arc quenching, and liquefaction have not yet been reported in the fields of applied physics and high-voltage engineering. The authors believe that a new insulating gas as an alternative to SF_6 can be discovered or developed, based on the physics-based knowledge of gas discharge.

5. Conclusions

This study investigated the surface discharge characteristics of epoxy resin in compressed gases, namely SF_6, dry air, and N_2, in a non-uniform electric field. Among the different gases, SF_6 and dry air, which are electronegative gases, revealed better insulation performances compared with N_2, owing to their electron attachment ability. The effect of electronegative gases on surface flashover voltages, varying with the pressure in these compressed gases, was analyzed in detail through the processes of electron attachment and electron detachment. Electron attachment induced an increase in the surface flashover voltage of the electronegative gas. Electron detachment seemed to result in saturation of the voltages as the pressure increased. A surface discharge mechanism that includes electron attachment, electron detachment, and secondary electron emission (SEEA and photoemission) was proposed for an analysis of the surface flashover voltages, which varied with the gas pressure. From this mechanism, it was found that the physical phenomena governing the behavior of electrons, including electron attachment, electron detachment, and electron scattering, are related to an improvement in the dielectric strength of the mixed gas. Based on these findings, techniques for improving the dielectric strength of mixed gases were discussed from a physics and engineering point of view. The discussions and knowledge of the physics behind gas discharge suggest the possibility of a new insulating gas to replace SF_6. To discover and develop the new insulating gas, theoretical and experimental attempts to understand the effects of varying the pressure on electron attachment and electron detachment are required. In addition to such attempts, the insulation characteristics of gases and mixed gases and their discharge mechanisms under DC and AC voltages must specifically be identified. This study contributes to explorations attempting to expand the knowledge of physics that governs gas discharge. The physical information obtained from the results of this study can be used to secure improved surface insulation performances by using the technique of mixing insulation gas in the surface insulation design of SF_6-free high-voltage equipment.

Author Contributions: Conceptualization, H.P., D.-Y.L. and S.B.; Investigation, H.P., D.-Y.L. and S.B.; Supervision, S.B.; Writing—original draft, H.P., D.-Y.L. and S.B.; Writing—review & editing, H.P., D.-Y.L. and S.B. All of the authors were involved in the preparation of the manuscript. All authors have read and agreed to the published version of the manuscript.

Funding: This research was funded by the Basic Science Research Program through the National Research Foundation of Korea (NRF) funded by the Ministry of Education, grant number 2017R1D1A3B03035693. This work was also supported by the Korea Institute of Energy Technology Evaluation and Planning (KETEP) grant funded by the Korea government (MOTIE) (No. 20192010107050).

Conflicts of Interest: The authors declare no conflict of interest.

References

1. Pan, B.; Wang, G.; Shi, H.; Shen, J.; Ji, H.-K.; Kil, G.-S. Green Gas for Grid as an Eco-Friendly AlternativeInsulation Gas to SF_6: A Review. *Appl. Sci.* **2020**, *10*, 2526. [CrossRef]
2. Xiao, S.; Zhang, X.; Tang, J.; Liu, S. A review on SF_6 substitute gases and research status of CF_3I gases. *Energy Rep.* **2018**, *4*, 486–496. [CrossRef]
3. Park, H.; Lim, D.-Y.; Bae, S. Partial discharge and surface flashover characteristics with O_2 content in N_2/O_2 mixed gas under a non-uniform field. *IEEE Trans. Dielectr. Electr. Insul.* **2018**, *25*, 1403–1412. [CrossRef]
4. Beroual, A.; Haddad, M.A. Recent Advances in the Quest for a New Insulation Gas with a Low Impact on the Environment to Replace Sulfur Hexafluoride (SF_6) Gas in High-Voltage Power Network Applications. *Energies* **2017**, *10*, 1216. [CrossRef]
5. Dunse, B.L.; Fraser, P.J.; Krummel, P.B.; Steele, L.P.; Derek, N. Australian HFC, PFC, Sulfur Hexafluoride and Sulfuryl Fluoride Emissions. Report Prepared for Australian Government Department of the Environment, by the Collaboration for Australian Weather and Climate Research, CSIRO Oceans and Atmosphere Flagship 2015, Aspendale, Australia, iv, 28. Available online: https://www.environment.gov.au/system/files/resources/71fad794-d98d-4014-95e6-53e9ce6493bf/files/australian-hfc-pfc-emissions-2015.pdf (accessed on 23 September 2020).
6. Mota-Babiloni, A.; Navarro-Esbrí, J.; Barragán-Cervera, Á.; Molés, F.; Peris, B. Analysis based on EU Regulation No 517/2014 of new HFC/HFO mixtures as alternatives of high GWP refrigerants in refrigeration and HVAC systems. *Int. J. Refrig.* **2015**, *52*, 21–31. [CrossRef]
7. California Air Resource Board, E.T.a.D.G.G.E. Electricity Transmission and Distribution Greenhouse Gas Emissions. Available online: https://ww2.arb.ca.gov/our-work/programs/elec-tandd (accessed on 23 September 2020).
8. Tsai, W.-T. The decomposition products of sulfur hexafluoride (SF_6): Reviews of environmental and health risk analysis. *J. Fluor. Chem.* **2007**, *128*, 1345–1352. [CrossRef]
9. Li, X.; Zhao, H.; Wu, J.; Jia, S. Analysis of the insulation characteristics of CF_3I mixtures with CF_4, CO_2, N_2, O_2 and air. *J. Phys. D Appl. Phys.* **2013**, *46*, 345203. [CrossRef]
10. Beroual, A.; Coulibaly, M.; Aitken, O.; Girodet, A. Investigation on creeping discharges propagating over epoxy resin and glass insulators in the presence of different gases and mixtures. *Eur. Phys. J. Appl. Phys.* **2011**, *56*, 30802. [CrossRef]
11. Goshima, H.; Okabe, S.; Ueda, T.; Morii, H.; Yamachi, N.; Takahata, K.; Hikita, M. Fundamental insulation characteristics of high-pressure CO_2 gas for gas-insulated power equipment—Effect of coating conductor on insulation performance and effect of decomposition products on creeping insulation of spacer. *IEEE Trans. Dielectr. Electr. Insul.* **2008**, *15*, 1023–1030. [CrossRef]
12. Li, Z.; Okamoto, K.; Ohki, Y.; Tanaka, T. The role of nano and micro particles on partial discharge and breakdown strength in epoxy composites. *IEEE Trans. Dielectr. Electr. Insul.* **2011**, *18*, 675–681. [CrossRef]
13. Li, S.; Huang, Y.; Min, D.; Qu, G.; Niu, H.; Li, Z.; Wang, W.; Li, J.; Liu, W. Synergic effect of adsorbed gas and charging on surface flashover. *Sci. Rep.* **2019**, *9*, 5464. [CrossRef] [PubMed]
14. Sadaoui, F.; Beroual, A. AC creeping discharges propagating over solid–gas interfaces. *IET Sci. Meas. Technol.* **2014**, *8*, 595–600. [CrossRef]
15. Sadaoui, F.; Beroual, A. DC creeping discharges over insulating surfaces in different gases and mixtures. *IEEE Trans. Dielectr. Electr. Insul.* **2014**, *21*, 2088–2094. [CrossRef]

16. Kato, K.; Kato, H.; Ishida, T.; Okubo, H.; Tsuchiya, K. Influence of surface charges on impulse flashover characteristics of alumina dielectrics in vacuum. *IEEE Trans. Dielectr. Electr. Insul.* **2009**, *16*, 1710–1716. [CrossRef]
17. Sudarshan, T.S.; Dougal, R.A. Mechanisms of Surface Flashover Along Solid Dielectrics in Compressed Gases: A Review. *IEEE Trans. Electr. Insul.* **1986**, 727–746. [CrossRef]
18. Li, C.R.; Sudarshan, T.S. Dielectric surface preflashover processes in vacuum. *J. Appl. Phys.* **1994**, *76*, 3313–3320. [CrossRef]
19. Lim, D.-Y.; Bae, S. Study on oxygen/nitrogen gas mixtures for the surface insulation performance in gas insulated switchgear. *IEEE Trans. Dielectr. Electr. Insul.* **2015**, *22*, 1567–1576. [CrossRef]
20. Douar, M.A.; Beroual, A.; Souche, X. Ignition and advancement of surface discharges at atmospheric air under positive lightning impulse voltage depending on perpendicular electric stress and solid dielectrics: Modelling of the propagating phenomenology. *Eur. Phys. J. Appl. Phys.* **2018**, *82*, 20801. [CrossRef]
21. Yan, X.; Zheng, Y.; Gao, K.; Xu, X.; Wang, W.; He, J. The Criterion of Conductor Surface Roughness in Environment-friendly C_4F_7N/CO_2 Gas Mixture. In Proceedings of the 2019 IEEE Sustainable Power and Energy Conference (iSPEC); Institute of Electrical and Electronics Engineers (IEEE), Bejing, China, 21–23 November 2019; pp. 377–381.
22. Nakano, Y.; Kojima, H.; Hayakawa, N.; Tsuchiya, K.; Okubo, H. Pre-discharge and flashover characteristics of impulse surface discharge in vacuum. *IEEE Trans. Dielectr. Electr. Insul.* **2014**, *21*, 403–410. [CrossRef]
23. Hikita, M.; Ohtsuka, S.; Okabe, S.; Kaneko, S. Insulation characteristics of gas mixtures including perfluorocarbon gas. *IEEE Trans. Dielectr. Electr. Insul.* **2008**, *15*, 1015–1022. [CrossRef]
24. Yializis, A.; Malik, N.; Qureshi, A.; Kuffel, E. Impulse Breakdown and Corona Characteristics for Rod-Plane Gaps in Mixtures of SF_6 and Nitrogen with Less Than 1% of SF_6 Content. *IEEE Trans. Power Appar. Syst.* **1979**, *5*, 1832–1840. [CrossRef]
25. Christophorou, L.G.; Olthoff, J.K. Electron Interactions with SF_6. *J. Phys. Chem. Ref. Data* **2000**, *29*, 267–330. [CrossRef]
26. Hosokawa, T.; Kaneda, T.; Takahashi, T.; Yamamoto, T.; Morita, T.; Sekiya, Y. DC breakdown characteristics in the gap with thin dielectric sheet in air. *IEEE Trans. Dielectr. Electr. Insul.* **2011**, *18*, 822–832. [CrossRef]
27. Raju, G.G. *Gaseous Electronics*; CRC Press: Boca Raton, FL, USA, 2012.
28. Teich, T.H. *Detachment of Electrons from Negative Ions in Electrical Discharges*; Springer Science and Business Media LLC: Boston, MA, USA, 1991; pp. 215–229.
29. Christophorou, L.; Pinnaduwage, L. Basic Physics of Gaseous Dielectrics. *IEEE Trans. Electr. Insul.* **1990**, *25*, 55–74. [CrossRef]
30. Qiu, X.Q.; Chalmers, I.D.; Coventry, P. A study of alternative insulating gases to SF_6. *J. Phys. D Appl. Phys.* **1999**, *32*, 2918–2922. [CrossRef]
31. Kojima, H.; Kinoshita, O.; Hayakawa, N.; Endo, F.; Okubo, H.; Yoshida, M.; Ogawa, T. Breakdown Characteristics of N_2O Gas Mixtures for Quasiuniform Electric Field under Lightning Impulse Voltage. *IEEE Trans. Dielectr. Electr. Insul.* **2007**, *14*, 1492–1497. [CrossRef]
32. Harris, J.R.; Kendig, M.; Poole, B.; Sanders, D.M.; Caporaso, G. Electrical strength of multilayer vacuum insulators. *Appl. Phys. Lett.* **2008**, *93*, 241502. [CrossRef]
33. Kurimoto, M.; Kato, K.; Hanai, M.; Hoshina, Y.; Takei, M.; Okubo, H. Application of functionally graded material for reducing electric field on electrode and spacer interface. *IEEE Trans. Dielectr. Electr. Insul.* **2010**, *17*, 256–263. [CrossRef]
34. Okubo, H. Enhancement of electrical insulation performance in power equipment based on dielectric material properties. *IEEE Trans. Dielectr. Electr. Insul.* **2012**, *19*, 733–754. [CrossRef]
35. Rokunohe, T.; Yagihashi, Y.; Endo, F.; Oomori, T. Fundamental insulation characteristics of air; N_2, CO_2, N_2/O_2, and SF_6/N_2 mixed gases. *Electr. Eng. Jpn.* **2006**, *155*, 9–17. [CrossRef]
36. Rokunohe, T.; Yagihashi, Y.; Aoyagi, K.; Oomori, T.; Endo, F. Development of SF_6-Free 72.5 kV GIS. *IEEE Trans. Power Deliv.* **2007**, *22*, 1869–1876. [CrossRef]